Experimental and Numerical Investigation about internal Cavitating Flow and Primary Atomization of a Large-Scaled VCO Diesel Injector with Eccentric Needle

T. Oda[*†], M. Hiratsuka, Y. Goda, S. Kanaike and K. Ohsawa
[*†] Department of Mechanical Engineering
Tottori University
Minami 4-101, Koyama, Tottori 680-8552 JAPAN

Abstract

An experimental and numerical study has been carried out to investigate the effects of eccentricity of a needle inside a valve-covered-orifice (VCO) diesel nozzle on internal cavitating flow and primary atomization, so that a 10 times large-scaled VCO nozzle was employed. Especially most of discusion focuses on the behavior observed at relatively low needle lift in this paper. The needle, which was incorporated into the nozzle, was manipulated by a three-dimensional traverse with micrometers. When the needle is perpendicularly positioned to the nozzle hole at low needle lift, trend of the spray cone angle becomes very complicated because of four regimes of cavitating flow inside the nozzle hole, in addition to the relatively high spray cone angle. In the same geometric condition, two regimes of primary atomization, the hollow cone spray regime and the solid cone spray regime, can be obtained. Reduction of spray cone angle is observed experimentally when atmospheric air is introduced from the hole entrance and the air-core (fully covered vortex cavitation) is produced inside the nozzle hole. The numerical simulation by using the Volume of Fluid (VOF) model can indicate the same phenomena.

Introduction

The valve-covered-orifice (VCO) nozzles are used due to reduction of unburned hydrocarbon emissions produced by diesel engines. However some researchers [1,2,3,4] have qualitatively demonstrated that different size sprays were ejected from real-size VCO nozzle because of eccentric location of needle incorporated into the nozzle. As a result, asymmetric combustion and soot formation are caused [1].

The large-scaled nozzles have been employed frequently, so that cavitation bubbles and resulting sprays could have been easily observed [5,6]. Especially, string-like bubbles, so called the vortex cavitation bubbles, and hollow cone sprays have been observed at very low needle lifts. We performed a steady-state experiment by using a 10 times large-scaled VCO nozzle with good spatial resolution of a 3-D traverse to manipulate a needle. As a result, the experimental study provided quantitative information that the eccentric location of needle influences behavior of cavitating flow inside the nozzle and spray cone angle of resulting liquid jets [7,8]. This experimental study seems to suggest that axial momentum and angular momentum of internal flow might play an important role in the flow pattern and the structures of liquid jets.

In this paper we present experimental results about effects of eccentric location of a needle on internal cavitating flow and primary atomization. Additionally, a three-dimensional computational fluid dynamic (CFD) simulation of cavitating flows by employing the Volume of Fluid (VOF) model was performed. Finally, internal cavitating flow and spray cone angle, which are obtained numerically at very low needle lifts, are compared with experimental results.

Experimental Procedure

An accumulator containing water, which was employed as the test liquid, was pressurized up to 1.2MPa. The liquid from the accumulator passed steadily through a needle valve and a Bourdon-type pressure gauge, which were used to control the injection pressure, before the liquid attained a nozzle holder, which is shown in Fig. 1. The liquid introduced into

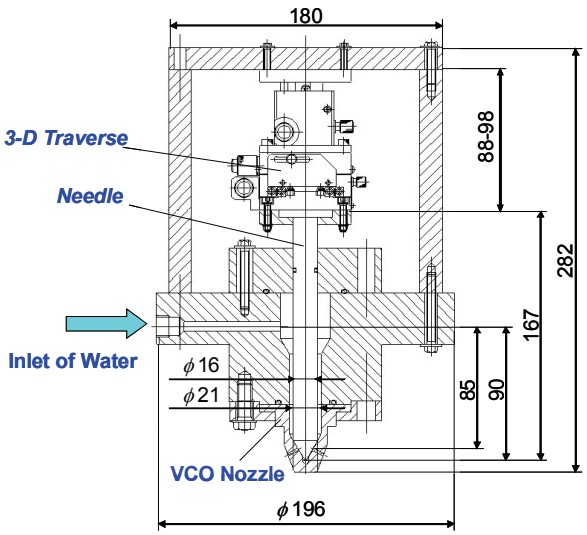

Figure 1. Schematic of nozzle holder with 10 times large-scaled VCO nozzle.

* Corresponding author: odate@mech.tottori-u.ac.jp

an inlet of the nozzle holder before flowing a pre-nozzle region which was located just upstream of a seat. A needle was incorporated into the nozzle holder, and had a diameter of 16mm and a 60°-edge tip. A large-scaled VCO nozzle, which was made of transparent acrylic resin, was mounted downstream of the nozzle holder. Finally the liquid was ejected from nozzle holes to the quiescent atmospheric air. The needle was mounted underneath the 3-D traverse with three micrometers which could provide a minimum resolution of 10μm. The needle lift and the eccentric radial location were set in terms of the micrometers reading before the liquid was emerged.

The large-scaled VCO nozzle had two nozzle holes as illustrated in Fig. 2 (a). Both the nozzle holes had sharp-edged circular shape at the entrance of the holes. The diameter of both the nozzle holes was 2mm and the length was 8mm, providing a length to diameter ratio of 4. The large-scaled VCO nozzle was ten times larger than real-size diesel nozzles. At an injection pressure of 0.20MPa the Reynolds number of the flow inside the nozzle hole of the large-scaled VCO nozzle was achieved at Reynolds number of approximately 40000. The Reynolds number of the large-scaled VCO nozzle was nearly the same value as that of real-size diesel nozzles. The needle lift and the radial location denote L_h and r, respectively. ϕ describes the azimuthal angle from common plane of the two holes axes. However our coordinate system is different from conventional cylindrical coordinate system. Figures 2 (b) and (c) explain radial locations at the azimuthal angle of 0^o and 90^o, respectively. The radial location which has negative value is opposed to that which has positive value in our coordinate system. There exists the radial location along the direction of the nozzle holes at the azimuthal angle of 0^o (Fig. 2 (b)). As the value of the radial location decreases at the azimuthal angle, the needle approaches the entrance of the nozzle hole for observation.

Cavitating bubbles inside the nozzle and liquid jet were illuminated simultaneously by two Xenon flashes of 4μs duration. Therefore front-lit photographs of cavitating bubbles and the liquid jet were captured by a digital still camera. Behaviors of the cavitating flow and the liquid jet breakup could be observed from each photograph, and spray cone angle was estimated by using the photograph.

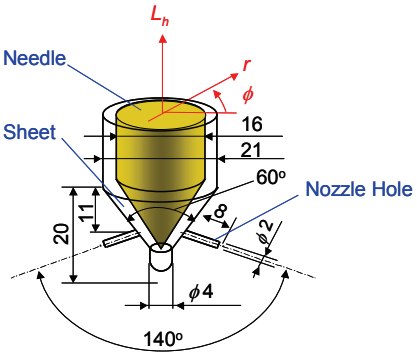

(a) Nozzle geometry and coordinate system

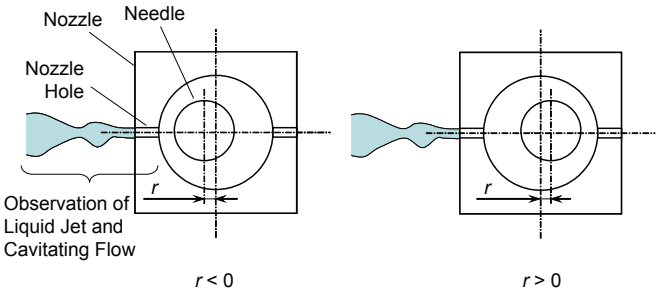

(b) Radial location of needle at azimuthal angle of 0^o

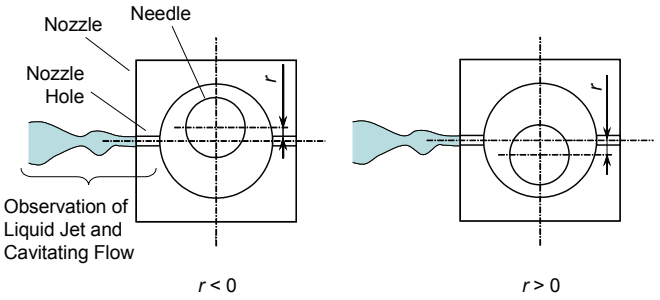

(c) Radial location of needle at azimuthal angle of 90^o

Figure 2. Schematic of nozzle geometry and coordinate system.

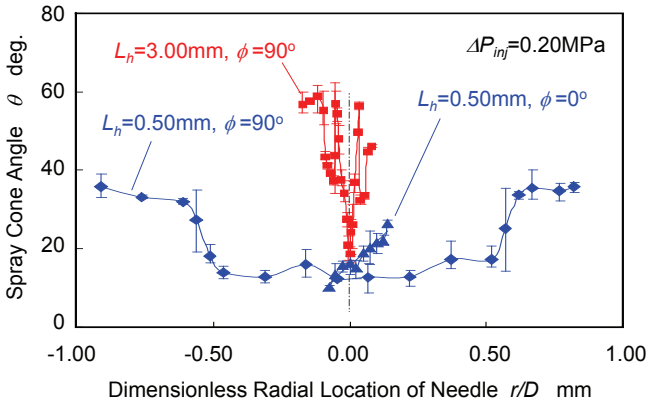

Figure 3. Effect of needle lift and azimthal on spray cone angle. (ϕ=90°, ΔP_{inj}=0.20MPa)

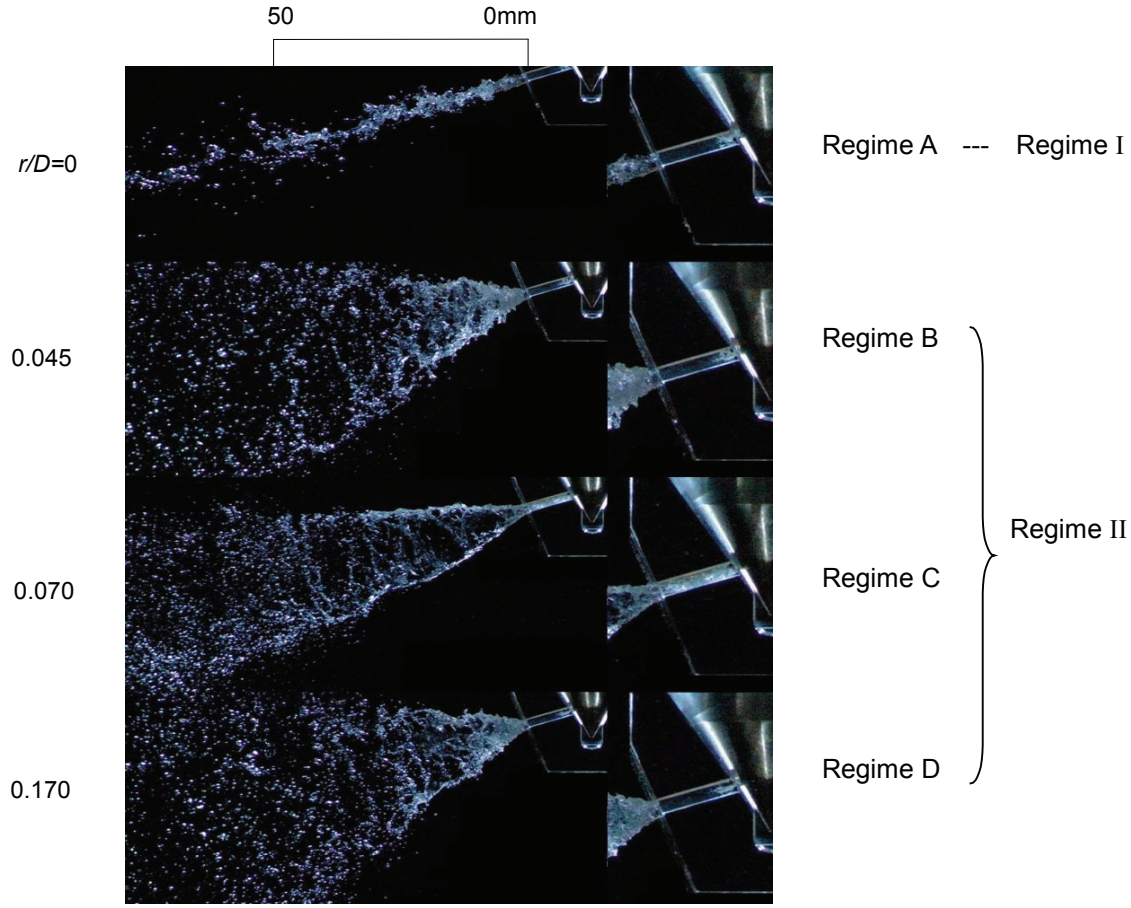

Figure 4. Effect of radial location of needle on cavitating flows inside nozzle hole (right photographs) and breakup behavior of liquid jets (left photographs). (ϕ=90°, ΔP_{inj}=0.20MPa, L_h=0.50mm)

Experimental Results

Figure 3 illustrates the effect of the needle lift and the azimuthal angle on the spray cone angles. At high needle lift of L_h =3.00mm the spray cone angle remains almost constant as the value of the radial location increases up to r/D=0.50. At the azimuthal angle of ϕ=90°, the spray cone angle increases significantly beyond r/D=0.50, so that the spray cone angle almost reaches maximum value. At the low needle lift of L_h=0.50mm measuring range of the radial location is smaller than that for L_h=3.00mm due to extremely smaller needle lift. In contrast to the trend at the high needle lift of L_h=3.00mm, the spray cone angle increases with increasing the value of the radial location monotonically. The significant increase of spray cone angle around the nozzle center must be caused by a narrow gap between the needle and the seat because of lower needle lift while the spray cone angle remains constant around the center at higher needle lift.

It is noted that the trend of the spray cone angle becomes very complicated at the low needle lift of L_h=0.50mm and the azimuthal angle of ϕ=90° and spray cone angle of this case is larger than that observed at other cases. This figure shows symmetry of the both profiles obtained at ϕ=90°, in contrast to the profiles obtained at ϕ=0°.

Two different breakup behaviors of liquid jets I and II are obtained as demonstrate in Fig. 4 obtained at the low needle lift of L_h=0.50mm and the azimuthal angle of ϕ=90° as follows: one is the solid cone spray/wavy jet regime (regime I) when the needle is located near the center of the nozzle(r/D=0), and another is the "hollow cone spray" regime (regime II) when the needle is located relatively far from the center of the nozzle (r/D=0.045, 0.070, 0.170). Many large droplets at the periphery of the hollow cone spray are yielded at the end of the conical liquid sheet.

Four regimes of cavitating flows are obtained by similar photographs to Fig. 4.

As the needle located near the center of the nozzle (Regime A: upperside and lowerside sheet cavitation, at r/D=0 in Fig. 4), bubble of the vortex cavitation can not be observed but bubbles of the sheet cavitation, which are yielded at upperside and lowerside of the entrance of the hole, can be observed. The spray cone angle increases with the value of radial location of the needle among the regime A as represented in Fig. 5. Regime B is the so-called transient regime (Upperside sheet cavitation and partial vortex cavitation, at r/D=0.045 in Fig. 4). Short bubble of the vortex cavitation is produced with bubbles of sheet cavitation at the entrance of the hole. The solid cone spray or the hollow cone spray can be appeared at the regime B. And then the bubble of the vortex cavitation is elongated and the tip of the bubble penetrates to the exit of the hole, so the "air-core" is produced (Regime C: fully covered vortex cavitation, at r/D=0.070 in Fig. 4). As results, the spray cone angle reaches peak value, and the spray cone angle significantly diminished. However the sheet cavitation can not be appeared any more. Finally, the bubble of the vortex cavitation becomes short as the needle is located enough far from a nozzle center in spite of relatively large spray cone angle (Regime D: partial vortex cavitation, at r=0.170 in Fig. 4).

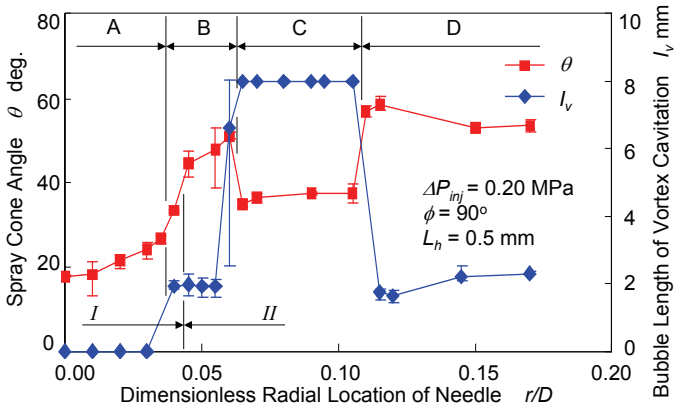

Figure 5. Effect of radial location of needle on spray cone angle and length of vortex cavitation. (ϕ=90°, ΔP_{inj}=0.20MPa, L_h=0.50mm)

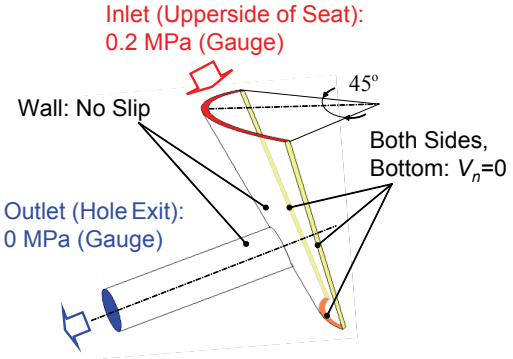

Figure 6. Schematic of the computational domain.

Numerical Methods

As mentioned above, spray cone angle is drastically varying with pattern of cavitating flow inside nozzle hole, when the needle is radially positioned in the direction perpendicular to both the holes and the nozzle has narrow gap between the needle and the seat. Especially, it seems possibly that the vortex cavitation is likely to influence the spray cone angle. Therefore remaining discussion will focus on the internal cavitating flows at the low needle lift of L_h=0.50mm and the azimuthal angle of ϕ=90°.

The CFD code STAR-CD version 4.02 has been used for this study. The code solved the three-dimensional compressible average Navier-Stokes equations, coupled with the realizable k-ε model [9] as a turbulent model. The simplified Rayleigh's model was employed for mass transfer which is caused evaporation of liquid and condensation of vapor at the surface of cavitating bubbles inside the nozzle. In addition, the simulations were done using Volume of Fluid (VOF) model to capture the formation of an air-core which are introduced from the hole exit.

The simulation was made within a domain shown in Fig. 6. For computational efficiency, a 45° sector of the test nozzle with one nozzle hole was modeled. Meshes were crated with total of about 1,700,000 cells. Particularly, high mesh density was used near the inner wall of the seat, the needle and the nozzle hole. The wall conditions with no-slip boundary conditions for velocity and zero gradient condition for pressure fields were imposed. The inlet pressure of the domain was set as 0.2MPa (gauge), and the outlet (exit of the nozzle

hole) pressure of the domain was set as 0MPa (gauge) in all cases. The ejecting liquid was only introduced from upside of the domain although the flow rate of the liquid from both sides and lower side of the domain was set to zero.

Spray cone angle was calculated as follows:

$$\theta = \tan^{-1} S \,. \qquad (1)$$

where S is swirl number which is numerically estimated from the axial and angular momentum of flow at the hole exit.

Numerical Results

Figure 7 exhibits a map of stream lines and a contour map of void fraction which are obtained by the numerical simulation. The map of stream linesindicates that ejecting liquid is forced to flow asymmetrically between the seat and needle due to displacement of needle as shown in Fig. 7 (a), so that the asymmetric flow produces rotating motion inside the nozzle hole. Finally the liquid emerges from the exit of the nozzle hole to the quiescent atmospheric air. Cavitation bubbles are apparent at the upperside and center of the hole

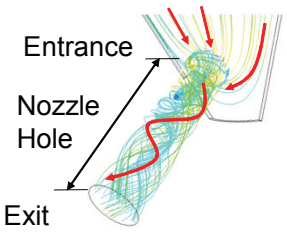

(a) Map of stream lines

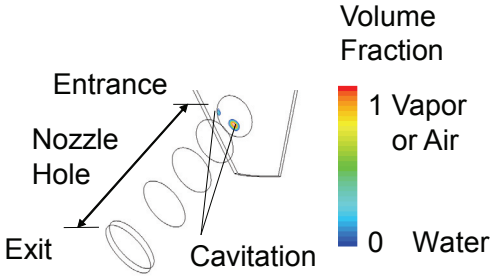

(b) Contour map of void fraction

Figure 7. Flow structure inside the nozzle. (ϕ=90°, ΔP_{inj}=0.20MPa, L_h=0.50mm, r/D=0.050)

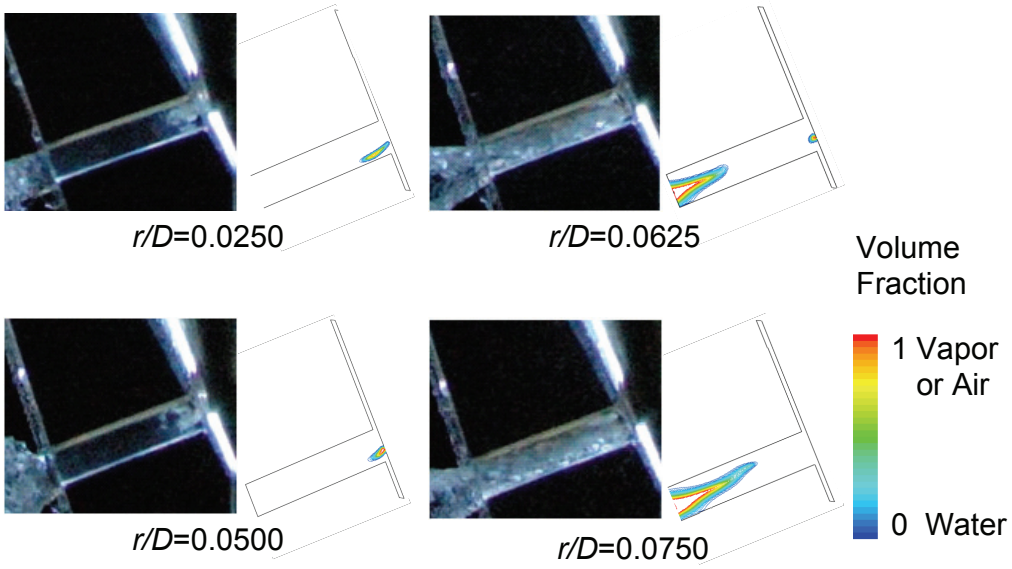

Figure 8. Effect of radial location of needle on cavitating flow and void fraction inside the nozzle hole. (ϕ=90°, ΔP_{inj}=0.20MPa, L_h=0.50mm)

entrance while bubbles can not be appeared at the hole exit in the contour map as illustrated Fig. 7 (b).

Figure 8 exhibits photographs of internal cavitating flow and contour maps of void fraction which are numerically obtained at a vertical plane with the hole axis. Entrance and exit of the nozzle hole are located at right-hand and left-hand side of each photograph, respectively. Although cavitating bubbles are produced in the vicinity of the upperside of the hole entrance at two radial locations, r/D=0.0250 and 0.0500, these bubbles are located out of the vertical plane to represent contour map. Thus no cavitating bubbles appear at the upperside of the hole entrance in these maps. Cavitating bubbles, which are obtained by using simplified Rayleigh's model, are appeared near the center of the hole entrance at r/D=0.1000 and 0.1500. In fact, in the regime B, a string-like short bubble, "core" of partial vortex cavitation, is observed at the hole entrance in the photograph. Usually, steady "core" of the vortex cavitation can be formed at the center of a swirling flow

where the pressure in the vortex core is often significantly small. Lower pressure leads to larger spherical bubbles and hence higher void fraction in the calculation, while the production of the short "core" is not taken in to account for the simulation.

Atmospheric air is introduced from the hole exit beyond r/D=0.0500, so that the air-core is created inside of the nozzle hole. In contrast to the fully covered vortex cavitation observed experimentally in the regime C, the length of air-core gradually increases with increasing the value of the radial location of needle, and finally the leading edge of the air-core reaches the needle. Figure 9 shows comparison of spray cone angle between the experimental and numerical results. The tendency of the predicted spray cone angle agrees well with measured up to about r/D=0.090. It is important to note that the numerical code can predict the peak angle around r/D=0.050. This numerical result indicates that the production of air-core corresponds to the reduction of spray cone angle. However, if the VOF model is not incorporated into calculation, this important result can not be obtained.

Conclusions

Experimental and numerical results about effects of eccentric location of a needle on internal cavitating flow and spray cone angle of a large-scaled valve-covered-orifice (VCO) diesel nozzle are presented. Especially we mainly focus the behavior at relatively low needle lift in this study.

(1) When the needle is perpendicularly positioned to the nozzle hole at low needle lift, trend of the spray cone angle becomes very complicated one because of four regimes of cavitating flow inside the nozzle hole, in addition to the relatively high spray cone angle.

(2) Two regimes of primary atomization, the hollow cone spray regime and the solid cone spray regime, can be obtained in the same geometric condition explained above.

(3) Reduction of spray cone angle of the hollow cone spray is observed experimentally when atmospheric air is introduced from the hole entrance and the air-core (fully covered vortex cavitation) is produced inside the nozzle hole.

(4) The numerical simulation by using the Volume of Fluid (VOF) model can indicate the same phenomena represented above.

Nomenclature

C_v	discharge coefficient
D	diameter of nozzle holes
L	hole length
L_h	needle lift
l_v	bubble length of vortex cavitation
r	radial location of needle
S	swirl number of internal flow of a nozzle hole
ΔP_{inj}	injection pressure
ϕ	azimuthal angle of eccentric needle
θ	spray cone angle

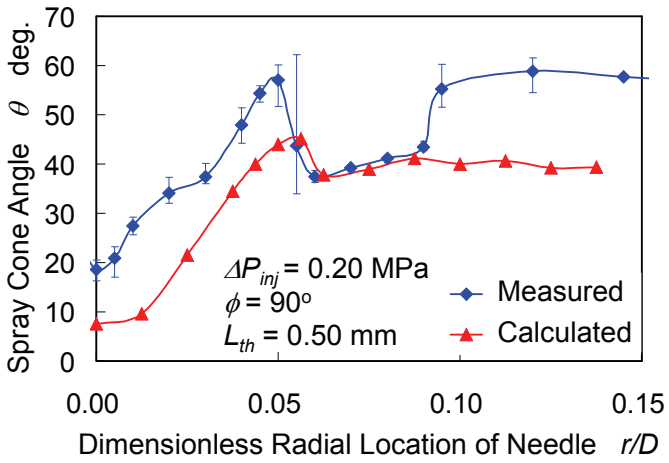

Figure 9. Comparison of spray cone angle between the experimental and numerical results. (ϕ=90°, ΔP_{inj}=0.20MPa, L_h=0.50mm)

Acknowledgements

The authors would like to thank Dr. T. Sumi for the technical support and comments. We also wish to thank Mr. K. Aoki and Mr. K. Ohnishi for helpful support.

References

[1] Renner, G, Koyanagi, K. and Maly, R. R., *Proc. the Fourth International Symposium on Diagnostics and Modeling of Combustion in internal Combustion Engines (COMODIA 98)*, pp. 477-482, 1998.

[2] Fettes, C., Heimgärtner, C. and Leipertz, A., *The Fifth International Symposium on Diagnostics and Modeling of Combustion in Internal Combustion Engines (COMODIA 2001)*, pp.54-59, 2001.

[3] Tsunemoto, H., Ishitani, H., Montajir, R., Hayashi, T., Kitayama, N., *The Fifth International Symposium on Diagnostics and Modeling of Combustion in Internal Combustion Engines (COMODIA 2001)*, pp.528-533, 2001.

[4] Kim, J. H., *Ph. D. Thesis*, University of Hiroshima, 2001 (in Japanese).

[5] Liverani, L., Arcoumanis, C., Yanagihara, H., Sakata, I. and Omae, K., *Proc. Seventh COMODIA International Symposium on Diagnostics and Modeling of Combustion in internal Combustion Engines*, JSME No.08-202, pp. 453-460.

[6] Kim, J. H. Nishida, K. and Hiroyasu H., *The 7th Internal Conference on Liquid Atomization and Spray Systems (ICLASS-'97) Proc.*, pp. 175-182, 1997.

[7] T. Oda, S. Kanaike, K. Aoki, Y. Goda and K. Ohsawa, *Proc. Of the 12th Annual Conference of ILASS-Asia and the 17th Symposium (ILASS Japan) on Atomization*, pp.21-26, 2008.

[8] T. Oda, Y. Goda, S. Kanaike, K. Aoki and K. Ohsawa, *Proceedings of the 11th Triennial International Annual Conference on Liquid Atomization and Spray Systems*, paper number: 132, 2009.

[9] T. H. Shin, et. al., *Computers and Fluids*, vol. 24, pp.227-238, 1995.